Co-Localization of Glycogen Synthase Kinase-3 with Neurofibrillary Tangles and Granulovacuolar Degeneration in Transgenic Mice

Takashi Ishizawa,* Narahiko Sahara,*
Koichi Ishiguro,[†] Jay Kersh,* Eileen McGowan,*
Jada Lewis,* Michael Hutton,* Dennis W. Dickson,*
and Shu-Hui Yen*

From the Department of Neuroscience,* Mayo Clinic Jacksonville, Jacksonville, Florida, and the Mitsubishi Kagaku Institute of Life Sciences,[†] Machida, Japan

Transgenic mice expressing human tau with P301L missense mutation (JNPL3) develop progressive amyotrophy, neurofibrillary degeneration, and neuronal loss. Mating of JNPL3 with transgenic mice expressing mutant amyloid precursor protein (Tg2576) leads to bigenic (TAPP) mice with enhanced neurofibrillary pathology. TAPP and JNPL3 mice were studied with immunocytochemistry and immunoblotting with antibodies to glycogen synthase kinase-3 (GKS3) to determine whether the development of tauopathy is associated with activation or increased expression of GSK3, and when the observed changes occur with respect to neurofibrillary tangle (NFT) formation. Accumulation of GSK3α/β phosphorylated at Y279/216 was observed in neurons containing NFTs and granulovacuolar degeneration (GVD), but not in normal neurons or neurons with pretangles. More GSK3 immunoreactive NFTs were detected in TAPP than JNPL3 mice, especially in the amygdala. These differences were notable only in old animals. There was no significant difference between animals with and without NFTs in the level of total, inactive, or Y216-phosphorylated (pY216)GSK3β. No apparent GSK3 accumulation was detected in neurons in Tg2576 mice. There was also no significant difference in the distribution of GSK3 in lysates fractionated based on their solubility in various reagents, including the sarkosyl-insoluble fraction. The results suggest that the pY216 GSK3β accumulates in NFT and GVD due to redistribution rather than increased expression or activation, and that pre-existence of tau abnormalities is required for APP/Aβ to exert their effects on tau pathology in TAPP mice. *(Am J Pathol 2003, 163:1057–1067)*

Neurofibrillary tangles (NFTs) and senile plaques are the two major histopathological lesions in Alzheimer's disease (AD). NFTs are composed of polymerized microtubule-associated protein tau.[1] Neurofibrillary lesions are also prominent features of progressive supranuclear palsy, corticobasal degeneration, Pick's disease and frontotemporal dementia and parkinsonism linked to chromosome 17 (FTDP17), which together are referred to as the tauopathies.[2] Several lines of transgenic mice have recently been generated that express wild-type or mutant human tau, and have been shown to develop tau abnormalities similar to those observed in humans.[3–8] Among them, mice expressing human four-repeat tau with no amino-terminal inserts (4R0N) and with P301L or with P301S mutation display robust neurofibrillary pathology.[5,8] In mice expressing P301L tau (referred to as JNPL3 mice), abnormal accumulation of tau is detected at as early as 3 months of age.[5] Most of the abnormal tau immunoreactive neurons are negative with Gallyas silver stain and are considered to be pretangles. As animals age, the number of Gallyas-positive NFT neurons increases. These NFTs were shown by immunoelectron microscopy to contain bundles of filamentous tau.[5] NFTs in JNPL3 mice were detected earlier in spinal cord than brain and were accompanied by a decrease in tau solubility characterized by resistance to extraction in detergents, such as Sarkosyl.[5,9] Bigenic mice generated by mating JNPL3 with Tg2576 mice, referred to as TAPP mice, which express P301L mutant tau and APP with so-called Swedish mutation (Lys[670]→ Asn, Met[671]→ Leu), developed both NFTs and amyloid plaques.[10] TAPP mice differed from JNPL3 by having enhanced neurofibrillary pathology in limbic regions, most notably the amygdala, suggesting a possible interaction between APP or amyloid and tau.[10]

The generation of NFT in both human neurodegenerative disorders and animal models is associated with phosphorylation of tau at multiple sites. Tau phosphory-

Table 1.   Antibodies

Antibody/antiserum	Species	Epitope	Source	Dilution	Reference
TPKI-C antiserum	Rabbit	29C-terminal amino acids	K. Ishiguro	1:500	20
TPKI/GSK3β PY216 antibody	Rabbit	Phosphorylated Tyr216	K. Ishiguro	1:500	45,46
pY279/216 antibody	Rabbit	Phosphorylated Tyr216	Biosource International	1:1000	22
TPKI/GSK3β-PS9 antibody	Rabbit	Phosphorylated Ser9 (inactive form)	K. Ishiguro	1:200	45,46
GSK3α/β monoclonal antibody	Mouse	Recombinant *Xenopus laevis* protein	Biosource International	1:500	47
CP13 monoclonal antibody	Mouse	Tau, phosphorylated at Ser 202 and Thr205	P. Davies	1:100	38
Ab39 monoclonal antibody	Mouse	Tau, conformation-dependent (NFT)	S. H. Yen	1:5	34
Tau-1 monoclonal antibody	Mouse	Tau, non-phosphorylated epitope located at 192–199	L J Binder	1:20	48

lation has been demonstrated to alter its conformation and could facilitate tau self-interaction.[11–14] A number of studies have documented that tau is a substrate of various kinases, including GSK3, cdk5/p25, JNK, ERK1/2, and p38, and that these kinases phosphorylate tau at sites similar to those identified in polymerized tau obtained from human and animal tissues.[15–18] Several kinases in their activated forms and GSK3β-phosphorylated tyrosine at amino acid residue 216 have been reported to co-localize with NFTs in AD as demonstrated by immunocytochemistry.[19–30] In addition, activation of GSK3β kinase has been detected in cultured cells treated with β amyloid peptides,[31,32] raising the possibility that activation or increased expression of kinase, or both, may play a significant role in the pathogenesis of tauopathies. These issues were addressed in the present studies by comparative analyses of JNPL3, TAPP, wild-type tau-transgenic mice, and non-transgenic mice at different ages with respect to the distribution as well as expression of inactive and pY216 GSK3β in spinal cord and brain, especially in the amygdala, which displays more tau pathology in 8-month and older TAPP mice than age-matched JNPL3 mice. Phosphorylation of GSK3β at serine 9 can lead to the inactivation of the kinase.[17] Although phosphorylation of GSK3β at tyrosine 216 (Y216) has been reported to be essential for its activity,[49] there are strong evidences from crystal structure studies to indicate that activity of GSK3β may not require the presence of phosphorylated Y216.[50] It remains possible that Y216 phosphorylation plays a role in facilitating substrate binding, since recombinant GSK3β fully phosphorylated at Y216 was reported to be more active than its unphosphorylated counterpart.[51]

Materials and Methods

Transgenic Mice

Transgenic mice and non-transgenic littermates were bred and genotyped for tau transgenes as described previously.[5,10] The number and age of mice studied for JNPL3 were four 4-month-old, two 5-month-old, six 6-month-old, two 7-month- old, seven 9-month-old, and one 14-month-old. Wild-type tau-transgenic mice were one each for 4-, 5.5-, 7-, and 15-month-old. TAPP mice were three 6-month-old, three 9-month-old, and one 11-month-old. Tg2576 mice were two 8-month-old, one 11-month-old, and one 15 month-old. Non-transgenic mice were one 2-month-old, four 3-month-old, three 9 month-old, one 12 month-old, and one 18-month-old. Only female mice were studied due to their increased susceptibility to tau abnormalities.[5,9,10]

Antibodies

The antibodies, their source and dilutions used in the present studies are listed in Table 1.

Gallyas Silver Stain and Immunoperoxidase and Immunofluorescent Labeling

Brains and spinal cords of mice were harvested, fixed in formalin, embedded in paraffin, and sectioned. The sections (5 μm in thickness) were mounted on microscopic slides, deparaffinized, and rehydrated as reported previously.[5] Some were subjected to Gallyas silver stain to reveal the presence of NFTs and neuropil threads, and these sections were counterstained with nuclear fast red. Others were treated further with periodic acid (0.5%, 10 minutes) and formic acid (98%, 30 minutes), microwaved for 15 minutes in 10 mmol/L citric acid buffer (pH 6.0), and incubated in 0.01 mol/L phosphate-buffered saline (PBS; pH7.4) containing 0.3% hydrogen peroxide (H_2O_2) for 20 minutes. They were then blocked in 5% normal horse or goat serum, and followed by incubation overnight or two nights at 4°C with primary antibody diluted in blocking solution. The slides were washed three times in PBS, incubated with anti-mouse or anti-rabbit secondary antibody (1:200, Vector ABC Elite kit; Vector Laboratories, Burlingame, CA) and then with avidin-biotin horseradish peroxidase (HRP) complex for 2 hours. The

presence of HRP was detected with 0.3 mg/ml 3,3′-diaminobenzidine (DAB) and 0.03% H_2O_2. The immuno-labeled sections were counterstained with hematoxylin. For studies of Tau-1 immunoreactivity, some sections were preincubated with a solution containing 10 U/ml of alkaline phosphatase (type III; Sigma, St. Louis, MO), 0.1 mmol/L $ZnCl_2$, 1.0 mmol/L $MgCl_2$, 1 mmol/L phenylmeth-ylsulfonyl fluoride (PMSF), 0.3 mg/ml dithiothreitol, and 100 mmol/L Tris-HCl at 37°C for 2 hours before incubation with the antibody.

After the completion of immunostaining with GSK3 antibodies, some sections were immersed in hematoxylin briefly for counterstaining and others were treated further with 0.1 mol/L glycine (pH 2.5) and 0.3% H_2O_2 solution in PBS for 20 minutes each, followed by treatment with 0.1 mg/ml proteinase K for 5 minutes at 37°C. The sections were then incubated with Ab39 antibody and the bound immunoglobulin was detected with Vector SG kit (1:100 dilution; Vector Laboratories), which produces a blue reaction product.

For immunofluorescent microscopy, the deparaffinized and rehydrated slides were incubated in a mixture of TPK1/GSK3$β$ PY216 and Ab39 diluted in blocking agent, followed by incubation in a mixture of Cy2- and Cy3-conjugated secondary antibodies (1: 100; Jackson Immunoresearch, West Grove, PA) for 2 hours at room temperature, washed three times, coverslipped in Aqua-mount (Lerner Laboratories, Pittsburgh, PA) and observed with confocal fluorescent microscope (Fluoview, Version 2.0; Olympus America Inc., Melville, NY). Some sections were labeled with Ab39 and thioflavin stain as reported previously.[10]

To investigate the specificity of anti-pY279/216, the antibody was absorbed with PHF-enriched sarkosyl-in-soluble fraction from an AD brain. CP13 absorbed with such a PHF preparation was used as a control. 600 $μl$ of anti-pY279/216 (1:1000) and CP13 (1:4000), respectively, were incubated overnight at 4°C with sarkosyl-insoluble fraction prepared from 150 mg wet weight of an AD brain (cortical region) and resuspended. The mixtures (volume = 615 $μl$) were centrifuged at 12,000 rpm (Eppendorf centrifuge) for 15 minutes. Supernatant containing the absorbed antibodies, and antibodies without the absorption were used to probe spinal cord sections from JNPL3 mice.

Tissue Extraction

Spinal cords and brains were removed immediately after the sacrifice of 6- to 10-month-old mice. Hemibrains were separated into cortico-limbic (cortex, amygdala, and hip-pocampus) and subcortical (basal ganglia, diencepha-lon, brain stem, and cerebellum) regions. The tissue was quickly frozen on dry ice and stored at −80°C. Each piece of frozen brain and spinal cord was weighed and homogenized in 5 volumes of Tris-buffered saline (TBS) containing protease and phosphatase inhibitors [25 mmol/L Tris/HCl, pH 7.4, 150 mmol/L NaCl, 1 mmol/L ethylenediaminetetraacetate (EDTA), 1 mmol/L EGTA, 5 mmol/L sodium pyrophosphate, 30 mmol/L $β$-glycero-phosphate, 30 mmol/L sodium fluoride, 1 mmol/L PMSF]. The homogenates were centrifuged in a Beckman TLA100.2 rotor (Beckman, Palo Alto, CA) at 150,000 × *g* for 15 minutes at 4°C. Supernatants were collected as SN1 fractions, and the pellets were re-homogenized in 5 volumes of high salt/sucrose buffer [0.8 mol/L NaCl, 10% sucrose, 10 mmol/L Tris/HCl (pH 7.4), 1 mmol/L EGTA, 1 mmol/L PMSF] and centrifuged as above. The superna-tants were incubated with sarkosyl (Sigma; 1% final concentration) for one hour at 37°C. The sarkosyl mixtures were then centrifuged in a Beckman TLA100.2 rotor at 150,000 × *g* for 30 minutes at 4°C. The supernatants and pellets were referred to as SN2 and P2 fractions, respectively. The pellets obtained after high salt and sucrose extraction were mixed with 5 volumes of RIPA buffer [containing 1% Triton X-100, 0.5% sodium deoxycholic acid, 0.1% sodium dodecyl sulfate (SDS) in TBS] for 30 minutes on ice, and centrifuged as described above to obtain RIPA-soluble (SN3) and -insoluble fractions. The RIPA-insoluble pellets were extracted with 5 volumes of 2% SDS and separated into SDS-soluble (SN4) and pellet (P4) fractions. The P4 fractions were resuspended in 5 volumes of TBS buffer. All fractions were processed fur-ther for Western blotting analysis.

Western Blotting

The amount of sample loaded per lane was based on the initial wet weight of frozen spinal cord (SN1: SN2: SN3: SN4: P2: P4 = 1: 2.5: 1: 2.5: 30: 10). The samples were separated by gel electrophoresis on 10% SDS-PAGE gels and transferred to nitrocellulose membranes (Bio-Rad, Hercules, CA). All blots were incubated with a blocking solution containing 5% nonfat milk, 0.1% goat serum and 0.1% Tween-20 in TBS, incubated with various antibodies, and washed as previously described.[5,9,33] The washed blots were incubated for 1 hour at room temperature with peroxidase-conjugated, goat anti-rabbit (1:4000, Chemicon, Temecula, CA), anti-mouse IgG (1:2000, Bio Rad, Hercules, CA), followed with washing and detection of bound antibodies with the enhanced chemiluminescence system (ECL plus; Amersham Bio-sciences, Piscataway, NJ). Immunoreactivity of GSK3 proteins was analyzed from scanned films using MCID software (Imaging Research Inc., Ontario, Canada). To compare the relative amount of GSK3 protein, the same amount of the SN2 fraction prepared from an AD brain was loaded as a control in all Western blot experiments. After the densities of the immunoreactive bands corre-sponding to GSK3$β$ were measured with MCID, the rela-tive amounts of GSK3$β$ protein in different blots were normalized with GSK3$β$ standard from the AD sample.

To test the specificity of antibodies in detection of phos-phorylated GSK3, duplicate electroblots containing sarko-syl-insoluble fractions (P2) derived from the cortico- and subcortico-regions of a TAPP mouse were used. One blot was incubated with 100 mmol/L Tris-HCl (pH 8.1), 0.1 mmol/L $ZnCl_2$, 1 mmol/L $MgCl_2$, 1 mmol/L PMSF, and 0.2 mmol/L dithiothreitol in the presence of 10 units/ml alkaline phosphatase (EC. 3.1.3.1. Type 3; *Escherichia coli*; Sigma)
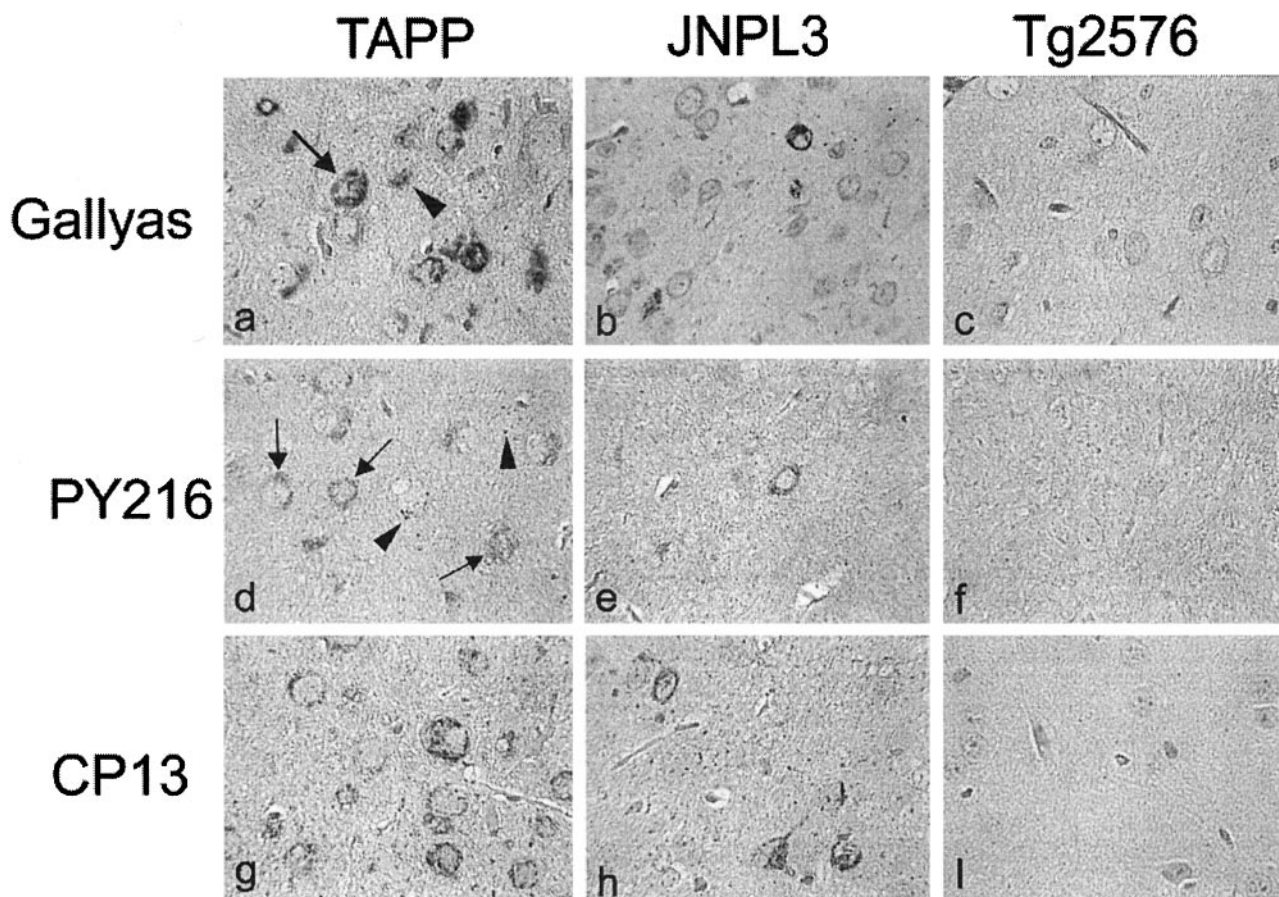
Figure 1. Localization of phosphorylated tau and GSK3α/β in the amygdala of TAPP, JNPL3, and Tg2576 mice. **a** to **c:** Gallyas silver stain and counterstaining with nuclear fast red. **d** to **f:** TPK1/GSK3β PY216 immunolabeling. **g** to **i:** CP13 immunolabeling; **d** to **f** and **g** to **i** were counterstained with hematoxylin. Gallyas silver stain showed NFTs in TAPP and JNPL3 mice (**a** and **b**) but not Tg2576 mice (**c**). TPK1/GSK3β PY216 immunoreactivity was located in neuronal cell bodies (marked with **arrow**) and GVDs (marked with **arrowhead**), but not neurites. Fewer TPKI/GSK3β PY216 immunoreactive cells were observed in JNPL3 (9-month-old) than TAPP mice (9-month-old), and none in Tg2576 (15-month-old). CP13 immunoreactive neurons and processes were detected in TAPP and JNPL3 mice and not in Tg2576 mice. Magnification: **a** to **i**, ×400.

for 4 hours at 37°C. The dephosphorylation was terminated by two 5-minute washes with PBS (pH 7.4). The second blot was not treated with phosphatase. Both blots were then probed with antibodies to Y216 phosphorylated form of GSK3.

Results

Tau Inclusions

Staining of brain and spinal cord sections with Gallyas silver stain revealed the presence of NFTs in JNPL3 and TAPP mice, but not in Tg2576 mice (Figure 1, a to c). NFTs in JNPL3 mice were more abundant in spinal cord than amygdala (Figures 1b and 2b). Both JNPL3 and TAPP mice were comparable in the extent of NFT in spinal cord, but the TAPP mice had more NFTs in the amygdala (Figure 1, a and b). The results are consistent with those previously reported.[10] Neurites positive with Gallyas silver stain were detected in neuropil of JNPL3 and TAPP, but not Tg2576 mice.

Immunolabeling with CP13 demonstrated phosphorylated tau in NFTs and pretangles in both JNPL3 and TAPP

mice, but not Tg2576 mice (Figure 1, g to i), wild-type human tau-transgenic mice or non-transgenic mice (data not shown). In comparison to JNPL3 mice, more NFTs and pretangles were detected in the amygdala of TAPP; however, the spinal cords were indistinguishable in terms of CP13 immunoreactivity. As reported previously, fewer neurons were positive with Gallyas silver stain than CP13, indicating that many of the CP13 immunoreactive neurons contain pretangles. Tau-1 immunoreactivity was not detected in JNPL3 (Figure 3b) or TAPP mice neurons (Figure 3d). NFTs became immunoreactive with Tau-1 on treatment of sections with alkaline phosphatase, indicating that the Tau-1 epitope was masked by phosphorylation. Unlike CP13, Tau-1 immunoreactivity was detected mainly in cell bodies and was not in pretangles (data not shown). The absence of Tau-1 immunoreactivity in neurites or pretangles suggests that the phosphorylation of Tau-1 epitopes and formation CP13 epitopes may not occur at the same time.

Expression of Phosphorylated GSK3

Immunostaining with anti-TPK1/GSK3β PY216 antibody showed labeling of some neurons in the spinal cord and
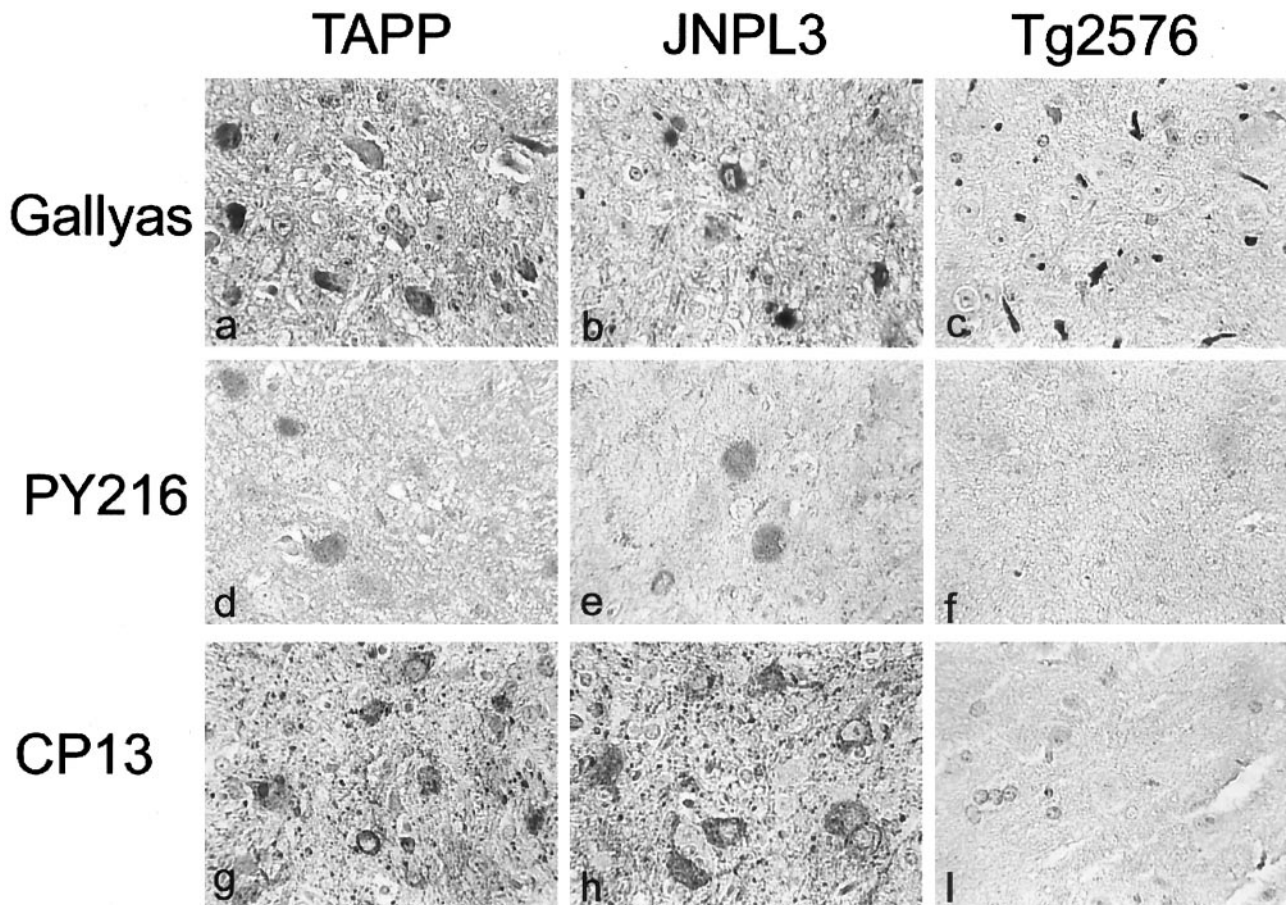
TAPP   JNPL3   Tg2576

Figure 2. Expression of phosphorylated tau and GSK3α/β in the spinal cord of TAPP, JNPL3, and Tg2576 mice. **a** to **c:** Gallyas silver stain. **d** to **f:** TPK1/GSK3β PY216 immunolabeling. **g** to **i:** CP13 immunolabeling. Gallyas silver stain demonstrates the presence of NFTs in TAPP and JNPL3 mice (**a** and **b**). Similar to that observed in brain sections, TPK1/GSK3β PY216 and CP13 immunoreactivities were located in neurons in the spinal cord of TAPP (9-month-old) and JNPL3 mice (9-month-old), and not in Tg2576 mice (15-month-old). In comparison to Gallyas silver stain and TPK1/GSK3β PY216 immunolabeling, more cells and processes display CP13-immunoreactivity. Magnification: **a** to **i**, ×400.

amygdala of both JNPL3 and TAPP mice. Either very weak or no immunolabeling was detected in cytoplasm of some neurons in Tg2576 mice and other controls. Unlike CP13 immunostaining, which revealed NFTs, pretangle, and neurites, pY216-positive GSK3 was located almost exclusively in neuronal cell bodies (Figures 1, d to f and 2, d to f). In some neurons in the amygdala and perirhinal cortex, GSK3 was detected in structures resembling granulovacuolar degeneration (GVD) (marked with arrowhead in Figures 1 and 4 for low and high magnification image). GVD were detected in the limbic regions, especially the amygdala of TAPP and to a lesser extent JNPL3 mice. Similar staining for GSK3 was also detected with another antibody raised to the tyrosine-phosphorylated form of GSK3 (Figure 4c, pY279/216) and two antibodies that recognize GSK3α/β and TPK1-C, irrespective of the state of GSK3 phosphorylation (Figure 4, d and e). In comparison, very little immunolabeling was detected in neurons or other cell types when tissue sections from transgenic mice were probed with antibodies to the inactive form of GSK3β (anti-TPK1/GSK3β PS9) (Figure 4f). Absorption of pY279/216 antibody with PHF-tau enriched preparations did not affect the immunoreactivity of the antibody with NFTs. In contrast, incubation of CP13
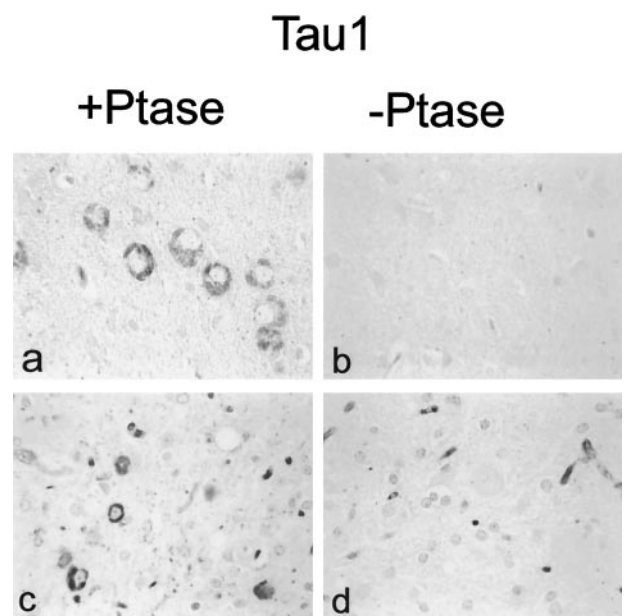
Tau1

+Ptase   -Ptase

Figure 3. Expression of the Tau-1 epitope. Tau-1 immunoreactivity was detected in brain (**a** and **b**) and spinal cord neurons (**c** and **d**) of TAPP and JNPL3 mice, respectively, and only in sections that had been pretreated with phosphatase (Ptase). Magnification: **a** to **d**, ×400.
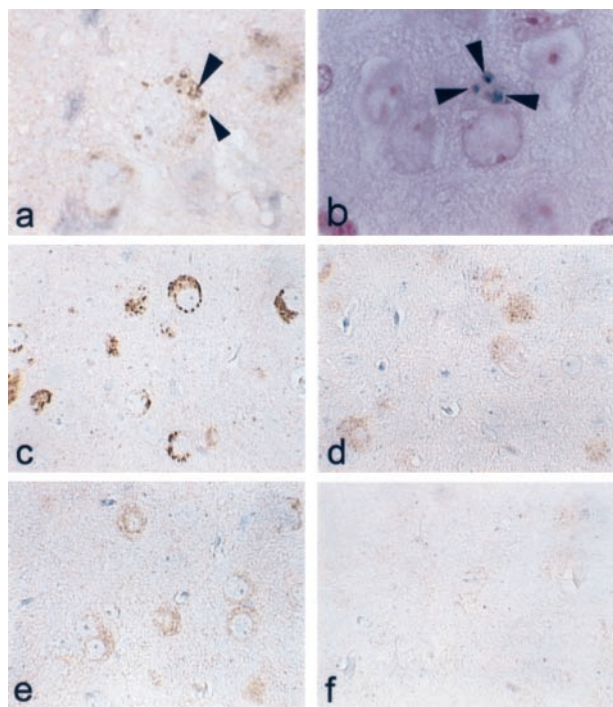
Figure 4. GSK3 immunoreactivity and Gallyas silver stain of GVD in TAPP mice. **a:** GVD displayed immunoreactivity with antibody TPK1/GSK3β PY216. **b:** GVD were positive with Gallyas silver stain. Neurons were labeled with antibodies pY279/216 (**c**), monoclonal GSK3α/β (**d**), and TPK1-C (**e**) but not with TPK1/GSK3-PS9 (**d**), an antibody to inactive GSK3. **Arrowheads** marked the GVD. Magnifications: **a** and **b**, ×1000; **c** to **f**, ×400.

with similar preparations removed most of the CP13 immunoreactivity, indicating the staining of NFT by pY279/216 is not due to cross-reactivity with phosphorylated tau (data not shown).

To confirm the type of neurofibrillary lesions that were immunoreactive for Y216 phosphorylated GSK3, sections were double-stained with TPK1/GSK3β PY216 (polyclonal) and Ab39, a NFT-specific monoclonal antibody, which recognizes conformational epitopes in NFT.[34] Ab39 detects late stages of neurofibrillary degeneration, and Ab39 immunoreactivity is absent from pretangles. GSK was not detected in neuronal cell bodies that were not labeled by Ab39 (data not shown). Similar results were obtained with confocal immunofluorescent microscopy; namely, both TPK1/GSK3β PY216 (green; Figure 5a) and Ab39 immunoreactivities (red; Figure 5b) were located in NFTs (Figure 5c), but not pretangles (Figure 5d). Neurofibrillary tangles labeled by Ab39 were thioflavin-S-positive (data not shown). In addition to NFTs, a fraction of neurites displayed GSK3 immunoreactivity (Figure 5, a and c), and these neurites were negative for Ab39 (Figure 5, b and c).

Temporal Accumulation of pY216 GSK3 Versus Phospho-Tau

Spinal cords of JNPL3 mice of different ages were compared for their immunoreactivity with CP13 and TPK1/GSK3β PY216. The results showed the presence of a detectable accumulation of CP13 immunoreactive phos-

pho-tau as early as 3 months of age (Figure 6), and increasing severity of tau pathology in older animals. In comparison, accumulation or expression of the active form of GSK3 was not detected until 5 months of age. Similar results were obtained withTPK1/GSK3β PY216 at three different dilutions (1:250, 1:500, and 1:1000) and with monoclonal GSK3 α/β antibody.

Analyses of GSK3 in Fractionated Tissue Extracts

Fractionated tissue extracts from JNPL3, TAPP, and non-transgenic mice of 6 to 9 months of age were analyzed by Western blotting to determine whether the accumulation of activated GSK3 was due to an increase in the amount of the kinase or alteration of the solubility of the kinase. All fractions contained three bands that were consistently labeled by two antibodies to the tyrosine-phosphorylated form of GSK3, anti-pY279/216 (Figure 7) and anti-TPK1/GSK3β PY216 (data not shown) as well as by antibodies to phosphorylation independent GSK3 (Figure 7C, c). The size of the immunoreactive proteins was consistent with GSK3α (53 kd) and GSK3β (two isoforms: 46 and 47 kd).[35] Immunoblotting with the antibody to the inactive form of GSK3β (pS9) showed very weak labeling of the bands with GSK3β immunoreactivity (Figure 7C, b), suggesting most GSK3β in tissue extracts is in an active state. Densitometric analysis of Western blots demonstrated that most GSK3β (both exon 8A+ and 8A- isoforms) was recovered in the SN1 fraction (Figure 7B). The proportion of GSK3β in different fractions is rank ordered as follows: SN1>SN2>SN3 ≥ SN4>P4>P2. JNPL3 mice tended to have lower total GSK3β and lower proportion of tyrosine-phosphorylated GSK3β in the P4 fraction (two of three) than non-transgenic mice; however, the differences were not statistically significant. No differences were observed between JNPL3 and TAPP mice (Figure 7C). To verify that anti-pY279/216 (or anti-TPK1/GSK3β PY216) recognizes phospho-GSK3, we compared the immunoreactivity of phosphatase-treated sarkosyl-insoluble fractions derived from a TAPP mouse with untreated fractions (Figure 8A). The results demonstrate that the immunoreactivity of GSK3 with anti pY279/216 antibody was reduced substantially by dephosphorylation.

A GSK3 immunoreactive band migrating at about 64 kd was detected only by the antibody to tyrosine-phosphorylated GSK3 (anti-pY279/216) purchased from Biosource International (Camarillo, CA) in the P2 (sarkosyl-insoluble) fraction derived from JNPL3 and TAPP, but not in corresponding fractions from non-transgenic or wild-type tau-transgenic mice [Figure 7A (P2) and C (d)]. This protein was weakly labeled in JNPL3 mice, and in brain samples it was detected mainly in those derived from subcortical regions. In comparison, a protein of this size was more intensely labeled in samples from the cortico-limbic regions of TAPP mice [Figure 7C (d)]. Cortico-limbic regions with more tau accumulation also displayed more 64-kd protein reactive with anti-pY279/216 GSK3. The results suggest that the level of this GSK3-reactive 64-kd protein is affected by transgenic expression of
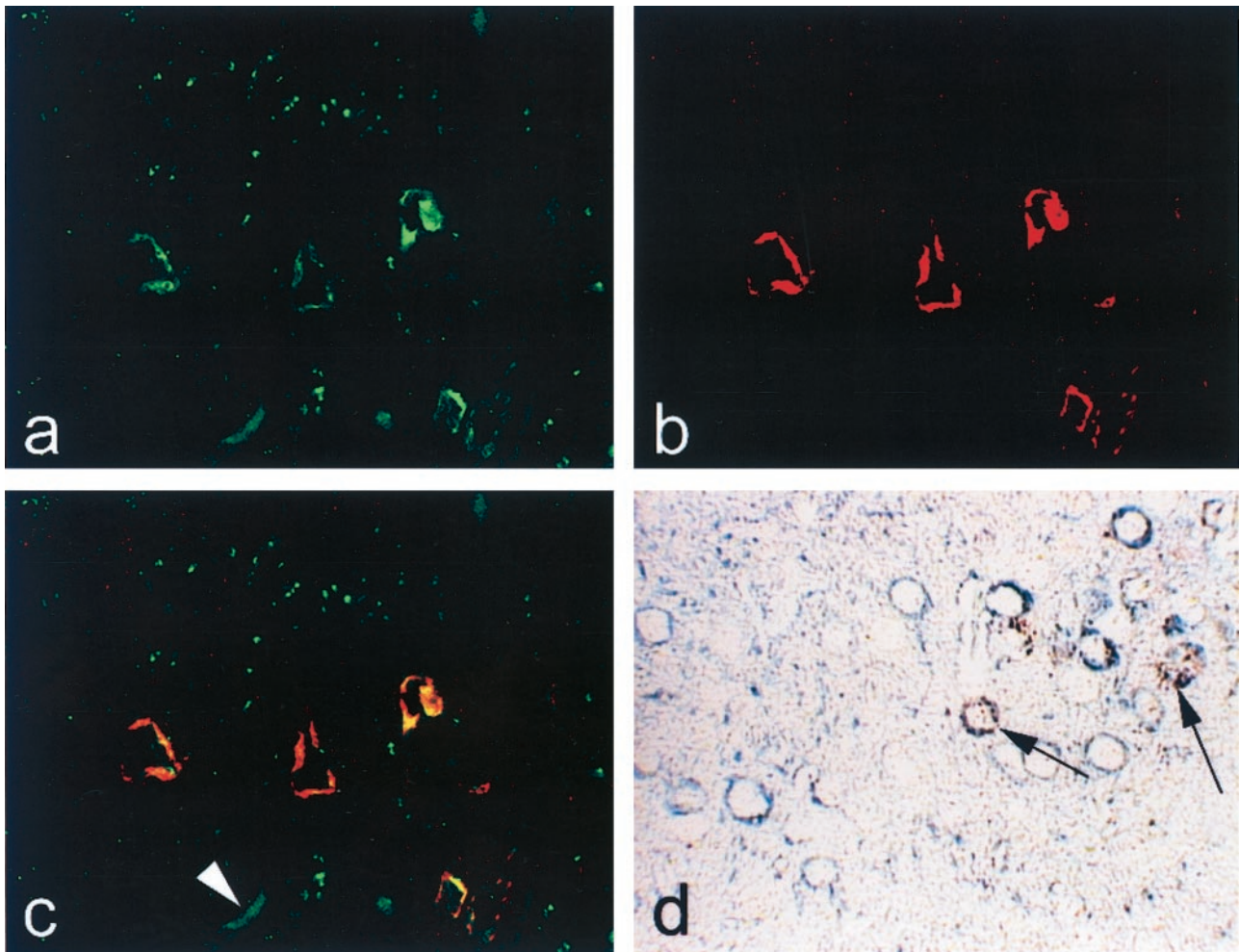
Figure 5. Dual labeling of brain sections with tau and GSK3 antibodies. pY216-positive GSK3 (**a**, green) were detected in NFTs reactive with Ab39 (**b**, red). **c:** Merged image of **a** and **b**. **Arrowhead** shows GSK3-positive/Ab39-negative neurites. **d:** Some CP13 reactive neurons were recognized by anti-pY216 (**arrow**). But many CP13 immunoreactive cell bodies and processes (blue) did not display immunoreactivity with the GSK3 antibody (brown). These neurons are at pretangle stages of development. Ab39 immunoreactive neurons were thioflavine-S-positive (data not shown). Magnifications: **a** to **c**, ×400; **d**, ×200.

APP/Aβ. Because the P2 fraction contains tau that migrates at about 64 kd, the possibility that the anti-pY279/216 antibody might cross-react with tau was examined by re-probing of GSK3 immunoblots with CP13 [Figure 7C (e)]. The pY279/216-positive 64-kd protein was found to comigrate with tau (64 kd), but its relative amount in cortico-limbic and subcortical regions were different from that of the tau-immunoreactive 64-kd protein [compare lanes 1 and 2 in TAPP, Figure 7C (d and e)]. Moreover, PHF-tau (sarkosyl-insoluble) from AD brains did not display pY279/216 immunoreactivity (Figure 8B), indicating that the anti-pY279/216 cross-reactive 64-kd protein is unlikely to be tau. Additional studies are needed to determine the molecular nature of this cross-reactive protein.

Discussion

GSK3 and several other kinases have been suggested to play a role in the pathogenesis of AD and related disorders with NFT.[19–30,36,37] This possibility was tested in our studies of transgenic animals with neurofibrillary lesions. Using antibodies specific to GSK3 to probe brain and spinal cord sections derived from JNPL3, TAPP, and control mice, we demonstrated that transgenic mice with NFTs differ from unaffected animals by containing neurons immunoreactive with antibodies reactive to GSK3α and GSK3β-phosphorylated at tyrosine located at amino acid residue 279 and 216, respectively. This form of kinase was located in a small fraction of neurons with phosphorylated tau, and these neurons were also positive with the Gallyas silver stain, thioflavin-S, and immunoreactive with Ab39. These results indicate that NFT-bearing neurons have abnormal accumulation of tyrosine-phosphorylated GSK3 and raise the possibility that formation of CP13 epitopes precedes the accumulation of GSK3 in the cell body. Tau-1 immunoreactivity was detected only in JNPL3 and TAPP mice sections treated with alkaline phosphatase, and the labeling was located in NFTs but not pretangles. Moreover, GSK3 phosphorylates Ser199 more readily than other kinases[15] and the Tau-1 epitope is located at amino acid residues
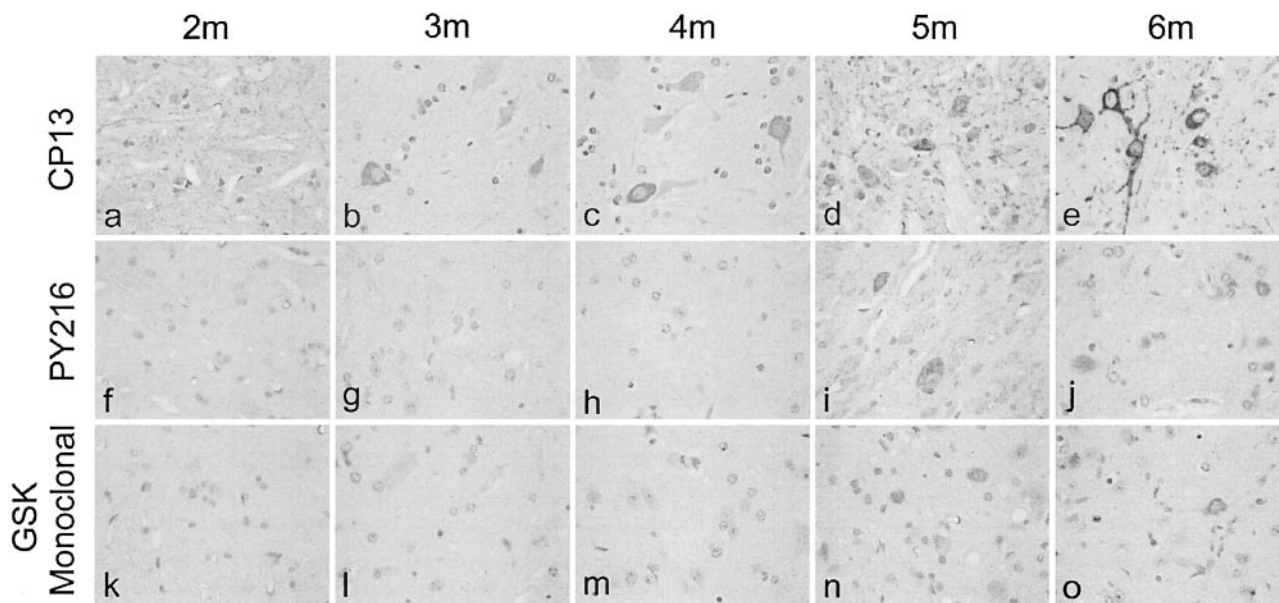
Figure 6. Immunolabeling of spinal cords from JNPL3 mice of various ages. CP13 immunoreactivity was detected in cell processes in 2-month-old mice, and in both cell bodies and processes in 3-month and older mice. In comparison, the immunoreactivity of pY216GSK3 was detected only in 5-month and older animals (see previous Figures, animals older than 6 months of age). m, month. Magnification: **a** to **o**, ×400

192–199.[39] The formation of the CP13 epitope probably requires the action of kinases such as ERK2, JNK, or p38, because each of these kinases has been shown to phosphorylate recombinant tau at Ser202 and Thr205,[15] which are epitopes recognized by CP13.[38] It is interesting to note that hyperphosphorylated tau-positive neurons in transgenic mice (5- to 6-month-old homozygous) expressing human P301S tau are reactive with antibodies to phosphorylated JNK and p38 kinase.[8]

Our finding that NFTs but not pretangles contained appreciable levels of GSK3 suggests that the association (sequestration) of GSK3 in NFT is not an early event in tau pathology, and it might occur in neurons after phosphorylated tau is aggregated in NFTs or when the concentration of activated GSK3 reaches a critical level. The lack of GSK3 immunoreactivity in pretangles, however, does not rule out the possibility that this kinase plays a role in abnormal tau formation, since continuous association between kinase and substrate is not essential for phosphorylation.

Antibodies specific to inactive form of GSK3β did not display immunoreactivities with phospho-tau-positive neurons in JNPL3 mice. It has been observed in two studies of AD brains that NFTs do not display inactive GSK3 immunoreactivity.[8,23] However, in a recent study, inactive GSK3 immunoreactivity was detected in many NFT in AD brains. It remains to be investigated whether the discrepancy is due to differences in the quality and specificity of the antibodies to inactive GSK3β or other factors. We have noted that the pS9 antibody reported to stain NFTs in AD brains labeled a band of molecular weight about 7 kd higher than that expected for GSK3β.[40]

Our immunolabeling of neuronal tissue with antibodies to GSK3 demonstrates that older TAPP mice are different from JNPL3 mice of similar ages, with TAPP mice displaying more robust GSK3 immunoreactivity in the amygdala. Age-matched Tg2576 mice did not display GSK3 immunoreactivity in neuronal cell bodies as seen in JNPL3 and TAPP mice. Since the TAPP mice with enhanced GSK3 immunoreactivity were not old enough to develop a significant number of amyloid plaques,[41] it seems reasonable to consider that Aβ oligomers or increased expression of APP, but not Aβ deposits, is associated with accumulation of tyrosine-phosphorylated GSK3 in NFTs. Moreover, since tau pathology was not observed in Tg2576 mice, a pre-existence of abnormal tau is likely required for APP or Aβ oligomers to exert their effects on tauopathy at least in the TAPP mouse model. In view of the accumulation of GSK3 immunoreactivity in NFT, but not in pretangles, we are tempted to speculate that the association of GSK3 with tau or phosphorylation of tau or other molecules by GSK3 may lead to stabilization of polymerized tau.

In JNPL3 and TAPP mice, GSK3 immunoreactivity was detected in GVD in addition to NFT. This result is comparable to that observed in a recent study of AD, in which GSK3β was located in GVD and a small proportion of NFTs.[42] It will be interesting to determine whether other kinases in active form are sequestered in NFTs and GVD in transgenic mice, and whether mouse GVD contain caspase-cleaved amyloid precursor protein as well as the activated form of caspase as demonstrated in AD and related disorders.[43,44] In an immunocytochemical study of brains staged for Alzheimer disease neurofibrillary changes, it was reported that pretangles contain tyrosine-phosphorylated form of GSK3.[22] Such immunoreactive neurons, however, may be undergoing granulovacuolar degeneration, since GSK3 immunoreactivities were located in granules similar to those observed in GVD.[22] Alternatively, the involvement of GSK3 in tauopa-
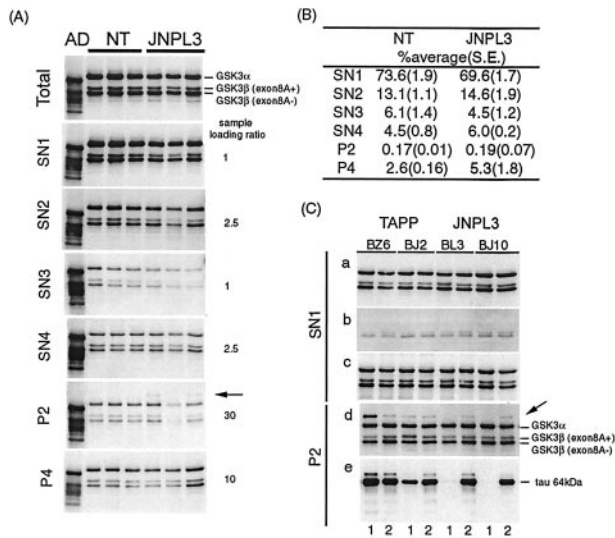
Figure 7. Partition of GSK3 in different samples derived from fractionated tissue extracts of non-transgenic, JNPL3, and TAPP mice. **A:** Unfractionated (Total) and fractionated samples (SN1-SN4, P2, P4) from spinal cords of three 9-month-old JNPL3 and 9-month-old non-transgenic (NT) mice were immunoblotted with anti-pY279/216 antibody. The sample loading was adjusted as indicated. SN2 fraction prepared from an AD brain (the first **lane** on each blot) was used as reference. GSK3 immunoreactivity was detected mainly in three bands of molecular weight consistent with GSK3α, and two isoforms of GSK3β (exon 8A+ and exon 8A-). Although JNPL3 samples tended to contain less GSK3 than non-transgenic controls, the differences were not statistically significant. Most GSK3 was recovered in the supernatant fraction (SN1) derived from high-speed centrifugation. PY279/216 immunoreactivity was also detected weakly in proteins of molecular weight about 64 kd (**arrow**) in the P2 (sarkosyl-insoluble) fraction. The band was not recognized by antibody TPK1/GSK3β PY216 (data not shown). **B:** Proportion of Y216-phosphorylated GSK3β in different fractions from spinal cords. Percentage of the mean was estimated after densitometric analysis of GSK3β immunoreactive band (46 and 47 kd in molecular weight). Standard errors were shown in parenthesis. **C:** Partition of GSK3 and phosphorylated tau in different regions of brains from JNPL3 and TAPP mice. Western blotting of SN1 fraction showed no differences between two JNPL3 (BL3, 9 months of age; BJ10, 9 months of age) and two TAPP (BZ6, 6 months of age; BJ2, 9 months of age) mice in the level of 279/216 phosphorylated GSK3α/β (**a**), inactive form of GSK3β (TPK1/GSK3β-PS9) (**b**), and total GSK3α/β (**c**) in the cortico-limbic (1) and subcortical (2) brain regions. Immunoblotting of the P2 fraction demonstrated the labeling of a band ~64 kd (**arrow**) by anti-pY279/216 antibody. This band was detected (**d**) mainly in the subcortical region in JNPL3 mice, and in both the cortico-limbic and subcortical regions in TAPP mice. Immunoblotting with CP13 showed (**e**) the labeling of 64 kd phosphorylated tau (tau 64 kd). In TAPP mice, the relative level of 64-kd protein in two brain regions detected by GSK3 antibody is higher than by phospho-tau antibody, suggesting that the GSK3 cross-reactive protein is probably not tau.

thies may be different between human and mutant tau-transgenic mice.

The data obtained from Western blotting demonstrate that the level of GSK3 (total, tyrosine-phosphorylated or inactive) was not significantly altered in transgenic mice with NFTs. Consistent with earlier studies,[45] our data showed that brain and spinal cord samples have weak immunoreactivity for the inactive form of GSK3, indicating that most GSK3 is constitutively active. Our analyses of fractionated tissue lysates also did not reveal significant differences in the partition of GSK3 in various fractions in mice with or without tau pathology. The lack of differences may reflect the fact that only a fraction of the neurons with abnormal tau accumulation have increased levels of GSK3. Alternatively, the differential display of GSK3 immunoreactivity in immunocytochemical studies
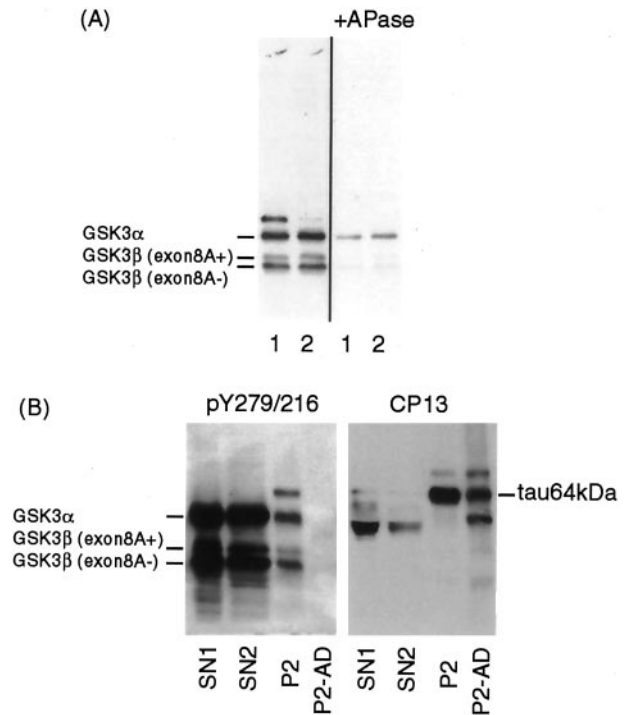

Figure 8. Western blotting demonstrating the specificity of anti-pY279/216 antibody. **A:** Replica electroblots containing sarkosyl-insoluble fractions (P2) prepared from the (1) cortico-limbic and (2) subcortical regions of a TAPP mouse were immunoblotted with anti-pY279/216 antibody. One blot was treated with alkaline phosphatase (10 units/ml) before incubation with the antibody. **B:** SN1, SN2, and P2 fractions derived from the cortico-limbic region of a TAPP mouse and a P2 fraction derived from AD brain were immunoblotted with anti-pY279/216 and reprobed with CP13. The amount of sarkosyl-insoluble mouse sample loaded per **lane** in **A** and **B** was derived from 2.4 mg of tissue. The amount of samples loaded per **lane** was based on the initial wet weight of frozen tissue (SN1: SN2: P2: P2/AD = 1: 5: 18: 15).

may be due to sequestration of GSK3 within NFTs instead of activation or increased expression of the kinase. It is worth noting that particulate fractions prepared from AD brains have been shown in a study to contain 30% to 40% less GSK3α and GSK3β than those from normal controls.[30] Such reduction in GSK3 may reflect the extensive neuronal loss in brains at advanced stages of AD.

In summary, we have found that GSK3 phosphorylated at tyrosine residue located in its activation segment is enriched in NFTs and GVD in transgenic mice expressing mutant human tau, and that sequestration rather than increased GSK3 expression or activation is the most likely basis for this observation. Finally, pre-existence of tau abnormalities may be required for APP or Aβ oligomers to have synergistic effects on neurofibrillary pathology in TAPP mice.

References

1. Grundke-Iqbal I, Iqbal K, Quinlan M, Tung YC, Zaidi MS, Wisniewski HM: Microtubule-associated protein tau: A component of Alzheimer-paired helical filaments. J Biol Chem 1986, 261:6084–6089

2. Lee VM, Goedert M, Trojanowski JQ: Neurodegenerative tauopathies. Ann Rev Neurosci 2001, 24:1121–1159

3. Ishihara T, Zhang B, Higuchi M, Yoshiyama Y, Trojanowski JQ, Lee VM: Age-dependent induction of congophilic neurofibrillary tau inclusions in tau transgenic mice. Am J Pathol 2001, 158:555–562

4. Götz J, Chen F, Barmettler R, Nitsch RM: Tau filament formation in transgenic mice expressing P301L tau. J Biol Chem 2001, 276:529–534

5. Lewis J, McGowan E, Rockwood J, Melrose H, Nacharaju P, Van Slegtenhorst M, Gwinn-Hardy K, Paul Murphy M, Baker M, Yu X, Duff K, Hardy J, Corral A, Lin WL, Yen SH, Dickson DW, Davies P, Hutton M: Neurofibrillary tangles, amyotrophy and progressive motor disturbance in mice expressing mutant (P301L) tau protein. Nat Genet 2000, 25:402–405

6. Probst A, Götz J, Wiederhold KH, Tolnay M, Mistl C, Jaton AL, Hong M, Ishihara T, Lee VM, Trojanowski JQ, Jakes R, Crowther RA, Spillantini MG, Bürki K, Goedert M: Axonopathy and amyotrophy in mice transgenic for human four-repeat tau protein. Acta Neuropathol 2000, 99:469–481

7. Spittaels K, Van den Haute C, Van Dorpe J, Bruynseels K, Vandezande K, Laenen I, Geerts H, Mercken M, Sciot R, Van Lommel A, Loos R, Van Leuven F: Prominent axonopathy in the brain and spinal cord of transgenic mice overexpressing four-repeat human tau protein. Am J Pathol 1999, 155:2153–2165

8. Allen B, Ingram E, Takao M, Smith MJ, Jakes R, Virdee K, Yoshida H, Holzer M, Craxton M, Emson PC, Atzori C, Migheli A, Crowther RA, Ghetti B, Spillantini MG, Goedert M: Abundant tau filaments and nonapoptotic neurodegeneration in transgenic mice expressing human P301S tau protein. J Neurosci 2002, 2:9340–9351

9. Sahara N, Lewis J, DeTure M, McGowan E, Dickson DW, Hutton M, Yen S-H: Assembly of tau transgenic animals expressing P301L tau: alteration of phosphorylation and solubility. J Neurochem 2002, 83:1498–1508

10. Lewis J, Dickson DW, Lin WL, Chisholm L, Corral A, Jones G, Yen SH, Sahara N, Skipper L, Yager D, Eckman C, Hardy J, Hutton M, McGowan E: Enhanced neurofibrillary degeneration in transgenic mice expressing mutant tau and APP. Science 2001, 293:1487–1491

11. Lu PJ, Wulf G, Zhou XZ, Davies P, Lu KP: The prolyl isomerase Pin1 restores the function of Alzheimer-associated phosphorylated tau protein. Nature 1999, 399:784–788

12. Zheng-Fischhofer Q, Biernat J, Mandelkow EM, Illenberger S, Godemann R, Mandelkow E: Sequential phosphorylation of tau by glycogen synthase kinase-3β and protein kinase A at Thr212 and Ser214 generates the Alzheimer-specific epitope of antibody AT100 and requires a paired-helical filament-like conformation. Eur J Biochem 1998, 252:542–552

13. Jicha GA, Lane E, Vincent I, Otvos L Jr., Hoffmann R, Davies P: A conformation- and phosphorylation-dependent antibody recognizing the paired helical filaments of Alzheimer's disease. J Neurochem 1997, 69:2087–2095

14. Daly NL, Hoffmann R, Otvos L Jr, Craik DJ: Role of phosphorylation in the conformation of tau peptides implicated in Alzheimer's disease. Biochemistry 2000, 39:9039–9046

15. Reynolds CH, Betts JC, Blackstock WP, Nebreda AR, Adnerton BH: Phosphorylation sites on tau identified by nanoelectrospray mass sprectroscopy: differences in vitro between the mitogen-activated protein kinases ERK2, c-Jun N-terminal kinase and P38, and glycogen synthase kinase 3β. J Neurochem 2000, 74:1587–1595

16. Lee VM, Goedert M, Trojanowski JQ: Neurodegenerative tauopathies. Ann Rev Neurosci 2001, 24:1121–1159

17. Planel E, Sun X, Takashima A: Role of GSK-3β in Alzheimer's disease pathology. Drug Development Res 2002, 56:491–510

18. Singh TJ, Zaidi T, Grundke-Iqbal I, Iqbal K: Modulation of GSK-3-catalyzed phosphorylation of microtubule-associated protein tau by non-proline-dependent protein kinases. FEBS Lett 1995, 358:4–8

19. Liu WK, Williams RT, Hall FL, Dickson DW, Yen SH: Detection of a Cdc2-related kinase associated with Alzheimer-paired helical filaments. Am J Pathol 1995, 146:228–238

20. Yamaguchi H, Ishiguro K, Uchida T, Takashima A, Lemere CA, Imahori K: Preferential labeling of Alzheimer neurofibrillary tangles with antisera for tau protein kinase (TPK) I/glycogen synthase kinase-3β and cyclin-dependent kinase 5, a component of TPK II. Acta Neuropathol 1996, 92:232–241

21. Vincent I, Jicha G, Rosado M, Dickson DW: Aberrant expression of mitotic cdc2/cyclin B1 kinase in degenerating neurons of Alzheimer's disease brain. J Neurosci 1997, 17:3588–3598

22. Pei JJ, Tanaka T, Tung YC, Braak E, Iqbal K, Grundke-Iqbal I: Distribution, levels, and activity of glycogen synthase kinase-3 in the Alzheimer disease brain. J Neuropathol Exp Neurol 1997, 56:70–78

23. Pei JJ, Braak E, Braak H, Grundke-Iqbal I, Iqbal K, Winblad B, Cowburn RF: Distribution of active glycogen synthase kinase 3β (GSK-3β) in brains staged for Alzheimer disease neurofibrillary changes. J Neuropathol Exp Neurol 1999, 58:1010–1019

24. Schwab C, DeMaggio AJ, Ghoshal N, Binder LI, Kuret J, McGeer PL: Casein kinase 1δ is associated with pathological accumulation of tau in several neurodegenerative diseases. Neurobiol Aging 2000, 21:503–510

25. Chin JY, Knowles RB, Schneider A, Drewes G, Mandelkow EM, Hyman BT: Microtubule-affinity regulating kinase (MARK) is tightly associated with neurofibrillary tangles in Alzheimer brain: a fluorescence resonance energy transfer study. J Neuropathol Exp Neurol 2000, 59:966–971

26. Zhu X, Raina AK, Rottkamp CA, Aliev G, Perry G, Boux H, Smith MA: Activation and redistribution of c-jun N-terminal kinase/stress-activated protein kinase in degenerating neurons in Alzheimer's disease. J Neurochem 2001, 76:435–441

27. Borghi R, Giliberto L, Assini A, Delacourte A, Perry G, Smith MA, Strocchi P, Zaccheo D, Tabaton M: Increase of cdk5 is related to neurofibrillary pathology in progressive supranuclear palsy. Neurology 2002, 58:5895–5892

28. Ferrer I, Blanco R, Carmona M, Puig B: Phosphorylated mitogen-activated protein kinase (MAPK/ERK-P), protein kinase of 38 kd (p38-P), stress-activated protein kinase (SAPK/JNK-P), and calcium/calmodulin-dependent kinase II (CaM kinase II) are differentially expressed in tau deposits in neurons and glial cells in tauopathies. J Neural Transm 2001, 108:1397–1415

29. Ferrer I, Blanco R, Carmona M, Ribera R, Goutan E, Puig B, Rey MJ, Cardozo A, Vinals F, Ribalta T: Phosphorylationed map kinase (ERK1, ERK2) expression is associated with early tau deposition in neurons and glial cells, but not with increased nuclear DNA vulnerability and cell death, in Alzheimer's disease, Pick's disease, progressive supranuclear palsy, and corticobasal degeneration. Brain Pathol 2001, 11:144–158

30. Baum L, Hansen L, Masliah E, Saitoh T: Glycogen synthase kinase 3 alteration in Alzheimer disease is related to neurofibrillary tangle formation. Mol Chem Neuropathol 1996, 29:253–261

31. Ferreira A, Lu Q, Orecchio L, Kosik KS: Selective phosphorylation of adult tau isoforms in mature hippocampal neurons exposed to fibrillar Aβ. Mol Cell Neurosci 1997, 9:220–234

32. Takashima A, Honda T, Yasutake K, Michel G, Murayama O, Murayama M, Ishiguro K, Yamaguchi H: Activation of tau protein kinase I/glycogen synthase kinase-3β by amyloid β peptide (25–35) enhances phosphorylation of tau in hippocampal neurons. Neurosci Res 1998, 31:317–323

33. Liu WK, Le TV, Adamson J, Baker M, Cookson N, Hardy J, Hutton M, Yen SH, Dickson DW: Relationship of the extended tau haplotype to tau biochemistry and neuropathology in progressive supranuclear palsy. Ann Neurol 2001, 50:494–502

34. Yen SH, Dickson DW, Crowe A, Butler M, Shelanski M: Alzheimer's neurofibrillary tangles contain unique epitopes and epitopes in common with the heat-stable microtubule-associated proteins tau and MAP2. Am J Pathol 1987, 126:81–91

35. Mukai F, Ishiguro K, Sano Y, Fujita SC: Alternative splicing isoform of tau protein kinase I/glycogen synthase kinase 3β. J Neurochem 2002, 81:1073–1083

36. Imahori K, Uchida T: Physiology and pathology of tau protein kinases in relation to Alzheimer's disease. J Biochem 1997, 121:179–188

37. Anderton BH, Betts J: Blackstock WP, Brion JP, Chapman S, Connell J, Dayanandan R, Gallo JM, Gibb G, Hanger DP, Hutton M, Kardalinou E, Leroy K, Lovestone S, Mack T, Reynolds CH, Van Slegtenhorst M: sites of phosphorylation in tau and factors affecting their regulation. Biochem Soc Symp 2001, 67:73–80

38. Jicha GA, Berenfeld B, Davies P: Sequence requirements for formation of conformational variants of tau similar to those found in Alzheimer's disease. J Neurosci Res 1999, 55:713–723

39. Liu W-K, Moore WT, Williams RT, Hall FL, Yen SH: Application of synthetic phospho- and unphospho-peptides to identify phosphorylation sites in a subregion of the tau molecule, which is modified in Alzheimer's disease. J Neurosci Res 1993, 34:371–376

40. Ferrer I, Barrachina M, Puig B: Glycogen synthase kinase-3 is associated with neuronal and glial hyperphosphorylated tau deposits in Alzheimer's disease, Pick's disease, progressive supranuclear palsy and corticobasal degeneration. Acta Neuropathol 2002, 104:583–591

41. Holcomb L, Gordon MN, McGowan E, Yu X, Benkovic S, Jantzen P, Wright K, Saad I, Mueller R, Morgan D, Sanders S, Zehr C, O'Campo K, Hardy J, Prada CM, Eckman C, Younkin S, Hsiao K, Duff K: Accelerated Alzheimer-type phenotype in transgenic mice carrying both mutant amyloid precursor protein and presenilin 1 transgenes. Nat Med 1998, 4:97–100

42. Leroy K, Boutajangout A, Authelet M, Woodgett JR, Anderton BH, Brion JP: The active form of glycogen synthase kinase-3β is associated with granulovacuolar degeneration in neurons in Alzheimer's disease. Acta Neuropathol 2002, 103:91–99

43. Su JH, Kesslak JP, Head E, Cotman CW: Caspase-cleaved amyloid precursor protein and activated caspase-3 are co-localized in the granules of granulovacuolar degeneration in Alzheimer's disease and Down's syndrome brain. Acta Neuropathol 2002, 104:1–6

44. Stadelmann C, Deckwerth TL, Srinivasan A, Bancher C, Bruck W, Jellinger K, Lassmann H: Activation of caspase-3 in single neurons and autophagic granules of granulovacuolar degeneration in Alzheimer's disease: evidence for apoptotic cell death. Am J Pathol 1999, 155:1459–1466

45. Planel E, Yasutake K, Fujita SC, Ishiguro K: Inhibition of protein phosphatase 2A overrides tau protein kinase I/glycogen synthase kinase 3β and cyclin-dependent kinase 5 inhibition and results in tau hyperphosphorylation in the hippocampus of starved mouse. J Biol Chem 2001, 276:34298–34306

46. Tomidokoro Y, Ishiguro K, Harigaya Y, Matsubara E, Ikeda M, Park JM, Yasutake K, Kawarabayashi T, Okamoto K, Shoji M: Aβ amyloidosis induces the initial stage of tau accumulation in APP$_{Sw}$ mice. Neurosci Lett 2001, 299:169–172

47. Demarchi F, Verardo R, Varnum B, Brancolini C, Schneider C: Gas6 anti-apoptotic signaling requires NF-kB activation. J Biol Chem 2001, 276:31738–31744

48. Binder LI, Frankfurter A, Rebhum LI: The distribution of tau in the mammalian central nervous system. J Cell Biol 1985, 101:1371–1378

49. Murai H, Okazaki M, Kikuchi A: Tyrosine dephosphorylation of glycogen synthase kinse-3 is involved in its extracellular signal-dependent inactivation. FEBS Lett 1996, 392:153–160

50. Dajani R, Fraser E, Roe M, Young N, Good V, Dale TC, Pearl LH: Crystal structure of glycogen synthase kinase 3β: Structural basis for phosphate-primed substrate specificity and autoinhibition. Cell 2001, 105:721–732

51. Kim L, Liu J, Kimmel AR: The novel tyrosine kinase ZAK1 activates GSK3 to direct cell fate specification. Cell 1999, 99:399–408